Lasers in Surgery and Medicine 40:273–281 (2008)

Multiphoton Excitation Fluorescence Microscopy of 5-Aminolevulinic Acid Induced Fluorescence in Experimental Gliomas

Sven Rainer Kantelhardt, MD,[1] Heike Diddens, PhD,[3] Jan Leppert, MD,[2] Veit Rohde, MD,[1] Gereon Hüttmann, PhD,[3] and Alf Giese, MD[1]*

[1]*Department of Neurosurgery, Georg-August-University of Göttingen, Robert-Koch-Strasse 40, 37075 Gottingen, Germany*

[2]*Department of Neurosurgery, University Hospital Schleswig-Holstein, Campus Luebeck, Ratzeburger Allee 160, 23538 Luebeck, Germany*

[3]*Institute of Biomedical Optics and Medical Laser Center GmbH, University Luebeck, Peter-Monnik-Weg 4, 23562 Luebeck, Germany*

Background and Objective: The clinical usefulness of 5-ALA guided detection of tumor tissue has been demonstrated for a number of malignancies. However, current techniques of intraoperative detection of protoporphyrin IX fluorescence in situ do not offer subcellular resolution. Therefore, discrimination of non-specific 5-ALA induced fluorescence remains difficult.

Materials and Methods: In this study we have used an orthotopic glioma model to analyze PpIX fluorescence in tumor tissue and normal brain by multiphoton excitation microscopy after intraperitoneal administration of 5-ALA. A DermaInspect in vivo imaging system was used for autofluorescence measurements at 750 nm excitation and detection in the green channel of a standard photomultiplier module. For detection of PpIX fluorescence at different excitation wavelengths a red sensitive version of the photomultiplier and a filter combination of short pass filters and a color glass long pass filter was used restricting the sensitivity in the red channel to a range of 580–700 nm.

Results: Multiphoton microscopy allowed a higher structural definition of tumor tissue based on the excitation of 5-ALA induced PpIX fluorescence compared to autofluorescence imaging. The high resolution of multiphoton microscopy allowed discrimination of fluorescence from the cytoplasm of tumor cells and 5-ALA induced PpIX fluorescence of normal brain parenchyma adjacent to tumor. Fluorescence lifetime imaging showed significantly longer fluorescence lifetimes of 5-ALA induced PpIX fluorescence in tumor tissue compared to normal brain. This allowed definition and visualization of the tumor/brain interface based on this parameter alone.

Conclusion: Multiphoton microscopy of 5-ALA induced PpIX fluorescence in brain tumor tissue conceptually provides a high resolution diagnostic tool, which in addition to structural information may also provide photochemical/functional information. Lasers Surg. Med. 40:273–281, 2008.

Key words: glioma; multiphoton excitation fluorescence microscopy; extent of resection; 5-ALA

INTRODUCTION

5-Aminolevulinic acid (5-ALA) is a naturally occurring intermediate of the heme biosynthesis [1]. Exogenous 5-ALA results in selective protoporphyrin IX (PpIX) accumulation in tumor cells including malignant gliomas to a greater extent compared to normal brain tissue [2–6]. 5-ALA induced fluorescence of PpIX, which has a maximum absorption around a wavelength of 400 nm, can be visualized by modified neurosurgical operating microscopes [7] and has shown to identify residual tumor during the resection of malignant gliomas in experimental and clinical settings [3,5,8]. After oral administration of 20 mg/kg 5-ALA, violet-blue light illumination produced an impression of intense red fluorescence in areas of viable tumor tissue or a faint (vague) pink fluorescence corresponding to varying degrees of tumor infiltration in tumor adjacent brain. In 42 malignant gliomas fluorescence was observed in 36 tumors. In fluorescent specimens from these tumors no tumor cells were found in six cases by conventional histology. In these false positive fluorescent samples five were found in areas of peritumoral edema or inflammatory cell and reactive astrocyte infiltration predominantly in recurrent gliomas [9]. Normal brain under illumination from modified operating microscopes showed no detectable fluorescence [5]. Low grade gliomas (WHO grade II) and low grade components of secondary malignant gliomas of WHO grade III and IV do not show detectable fluorescence by operating microscopes. Tumor necrosis due to the lack of viable cells and sufficient synthesis of PpIX

Contract grant sponsor: Future Investment Program of Schleswig-Holstein; Contract grant sponsor: Head and Neck Cancer Research Foundation, Wiesbaden, Germany; Contract grant sponsor: Novartis Foundation for Clinical Research, Nürnberg, Germany.

*Correspondence to: Prof. Alf Giese, MD, Department of Neurosurgery, Georg-August-University of Göttingen, Robert-Koch-Strasse 40, 37075 Gottingen, Germany.
E-mail: alf.giese@med.uni-goettingen.de

Accepted 1 February 2008
Published online in Wiley InterScience (www.interscience.wiley.com).
DOI 10.1002/lsm.20623

may also show no fluorescence. A recent randomized multicentre phase III trial demonstrated that fluorescence-guided resection of malignant gliomas using 5 ALA-induced porphyrins enables more complete resections of contrast-enhancing tumor and leads to an improved progression-free survival [10]. The clinical usefulness of 5-ALA guided detection of tumor tissue has also been demonstrated for bladder cancer [11–13], malignancies of the oral cavity [14,15] and the lung [16], the female genital tract [17,18], intraperitoneal metastases [19,20] the gastrointestinal mucosa [21] and skin [22]. However, current techniques of intraoperative detection of PpIX fluorescence do not offer subcellular resolution. Therefore, discrimination of non-specific fluorescence or PpIX synthesis by normal tissue remains difficult.

We have recently demonstrated that multiphoton excitation microscopy allows structural and photochemical imaging of human brain tumor tissue and central nervous system histoarchitecture at a subcellular level in unprocessed tissue blocks ex vivo [23]. Multiphoton excitation microscopy is based on the excitation of intra—and extracellular fluorophores by near-infrared femtosecond laser pulses focused to a femtoliter target volume [24]. The auto-fluorescence of native tissue is recorded by a photomultiplier and fluorescence intensity images or images of the fluorescence lifetime distribution may be reconstructed. In experimental gliomas and specimens of human malignant brain tumors solid tumor, the tumor/brain interface, and single invasive tumor cells could be visualized based on the excitation of endogenous fluorophores [23]. The analysis of the excitation/fluorescence lifetime profiles within specific excitation volumes discriminated glioma cells and normal brain cells [25]. The resolution and structural definition of multiphoton microscopy was sufficient to determine residual tumor tissue in specimens taken from the edge of the resection cavity during surgical removal of human brain tumors [25].

In this study we have used an orthotopic glioma model to analyze PpIX fluorescence after oral administration of 5-ALA in tumor tissue and normal brain by multiphoton excitation microscopy. Multiphoton microscopy allowed a higher structural definition of tumor tissue based on the excitation of PpIX fluorescence compared to autofluorescence imaging. Fluorescence lifetime imaging showed significantly longer fluorescence lifetimes of tumor tissue than normal brain, which allowed definition of the tumor/brain interface based on this parameter alone.

MATERIAL AND METHODS

Multiphoton Microscopy

Multiphoton exitation images were obtained using a DermaInspect in vivo imaging system (JenLab, Jena, Germany). The principle set-up is shown in Figure 1. The system contains a solid-state, mode-locked 80 MHz titanium:sapphire laser (MaiTai, Spectra Physics, Darmstadt,

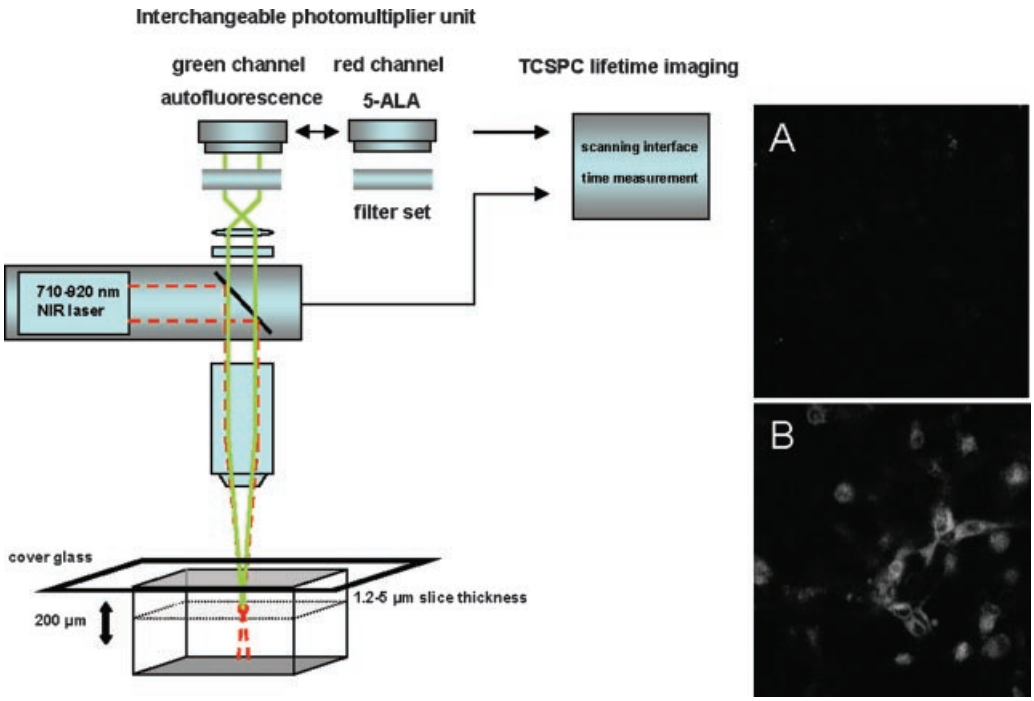

Fig. 1. Principle set-up of multiphoton excitation fluorescence microscopy of 5-aminolevulinic acid induced fluorescence. **A**: Autofluorescence was detected in the green channel of a photomultiplier after passing a beam splitter and a short-pass filter. **B**: PpIX fluorescence was detected using a red sensitive version of the photomultiplier and a filter combination of short pass filters 680 and 750 nm and a color glass long pass filter, which restricted the sensitivity in the red channel to a range of 580–700 nm and suppressed the excitation intensity.

Germany) with a tuning range of 710–920 nm, a mean laser output of >900 mW at 800 nm, and a 75 fs pulse width. Autofluorescence measurements were performed at 750 nm, which we have determined optimal for imaging of native brain and brain-tumor tissue in previous studies [23,25]. The scanning module contains a motorized beam attenuator, a shutter, and a two axis galvoscanner. A piezodriven 40× focussing optic (*z*-axis) with NA 1.3 and 140 μm working distance (Plan-Neofluar 40X, 1.3 oil, Zeiss, Göttingen, Germany) was used. Motions of *x*- and *y*-axis were performed by computer-controlled stepper-motors (Owis GmbH, Staufen, Germany). The signal of the autofluoresphores was detected in the green channel by a standard photomultiplier module (H7732, Hamamatsu, Herrsching, Germany), after passing a beam splitter (Chroma 640 DCSPXR, AHF analysentechnik AG, Tübingen) and a short-pass filter (BG39, Schott, Mainz, Germany). This gave a detection bandwidth from 350 to 590 nm. For detection of PpIX fluorescence at different excitation wavelengths a red sensitive version of the photomultiplier (H7732-10, Hamamatsu) and a filter combination (beamsplitter Chroma 725DCSPXR, AHF analysentechnik AG, Tübingen, LCLS-700-S, Laser Components, Olching, Germany), two custom made short pass filters 680 and 750 nm, and the color glass long pass filter OG590 (Schott), which restricted the sensitivity in the red channel to a range of 580–700 nm and efficiently suppressed the excitation intensity, were used.

Time-Resolved Autofluorescence Measurements

Fluorescence lifetime images were measured by time correlated single photon counting. Start signals from the photomultiplier (R928, Hamamatsu) and stop signals provided by the laser were processed by a PC based single-photon counting board (SPC 830, Becker & Hickl, Berlin, Germany), which allowed count rates of up to 8×10^6 photons/second. The single-photon counting board was synchronized with the spatial beam position, which was calculated from signals of the galvoscanner. Spatially resolved autofluorescence decay curves were recorded for 256×256 pixels per image field, which typically were 150 μm. The depth of the excitation volume was 0.5 μm. Curve fitting of a single exponential decay curve including a deconvolution with the time response of the system (SPCImage 2.6, Becker & Hickl) was used to calculate a mean fluorescence lifetimes for each pixel, which was displayed in color-coded images [26].

Glioma Cell Lines

The human glioblastoma derived cell line G-112 was propagated in monolayer culture in MEM containing 10% FCS. The human Leukemia cell line CCRF-CEM was maintained in suspension culture in RPMI 1640 containing 10% FCS. To induce PpIX fluorescence subconfluent monolayer cultures were incubated in a humidified atmosphere containing 5% CO_2 at 37°C in 1 mM 5-ALA in PBS for 4 hours. The cultures were rinsed in PBS and subjected to fluorescence analysis after cell viability was determined greater than 85% by the trypan exclusion test.

Orthotopic Glioma Mouse Model

The human glioblastoma derived cell lines G-112 and U87 were grown in MEM containing 10% FCS. For intracranial implantation in nude NMRI mice cells were harvested from monolayer culture by trypanization. Cells were washed and resuspended at a concentration of 2×10^4/μl. All procedures were performed in accordance with regulations of the Animal Care and Use Committee of the University Hospital of Schleswig-Holstein under permit No. 30/o/03. Prior to the implantations animals were anaesthetized by peritoneal injection of ketamine/xylazine solution (200 mg ketamine and 20 mg xylazine in 17 ml of saline) at 0.15 mg/10 g of body weight. For the procedure the cranium was fixed in a stereotactic frame (TSE Systems, Bad Homburg, Germany). A 1 mm bur hole was placed 3 mm lateral to the bregma and a stereotactic implantation of 3 μl cell suspension injected over 3 minutes was placed in an area corresponding to the internal capsule 0.5 mm below the fiber tracts of the corpus callosum. Following implantation 50 mg/kg novaminsulfone was administered s.c. and 1 mg/ml novaminsulfone was added to the drinking water for 3 days. Four weeks post implantation intraperitoneal 125 mg/kg 5-ALA (in 750 μl buffer, pH 7; Medac, Wedel, Germany) was administered. After 4 hours tumor bearing brains were explanted following a lethal intraperitoneal injection of 50 mg/kg xylazine and 350 mg/kg ketamine. Coronal sections of the mouse brains were performed immediately and the tissue samples were placed in a humidified chamber (MiniCeM, JenLab, Jena, Germany) adherent to a 0.17 μm cover glass for imaging. G-112 gliomas in mouse brain are highly invasive, typically invading the deep white matter and the corpus callosum indicating a high affinity of single invasive cells to myelinated fiber tracts. In contrast U87 gliomas show a well delineated expansive growth pattern with little invasion of adjacent brain [23].

RESULTS

Detection of Protoporphyrin IX Fluorescence by Multiphoton Microscopy

Using a standard version of the photomultiplier, at an excitation wavelength of 750 nm no protoporphyrin IX fluorescence of glioma cells in monolayer culture could be detected due to the low sensitivity in the emission range of PpIX (Fig. 1). To detect protoporphyrin IX fluorescence, which has a wavelength between 610 and 730 nm, the red channel with the special red-sensitive version of photomultiplier module and additional filters, which suppressed the excitation wavelength below 770 nm, was necessary. As expected from the one-photon absorption spectrum, excitation at 800 nm resulted in optimal intensity of cytoplasmic fluorescence immediately after administration of 50 mg/ml 5-ALA to monolayer glioma cultures (Fig. 2).

Multiphoton Microscopy of 5-ALA Induced Fluorescence in Experimental Gliomas

When mouse brains bearing the highly invasive G-112 experimental glioma were explanted 4 hours after

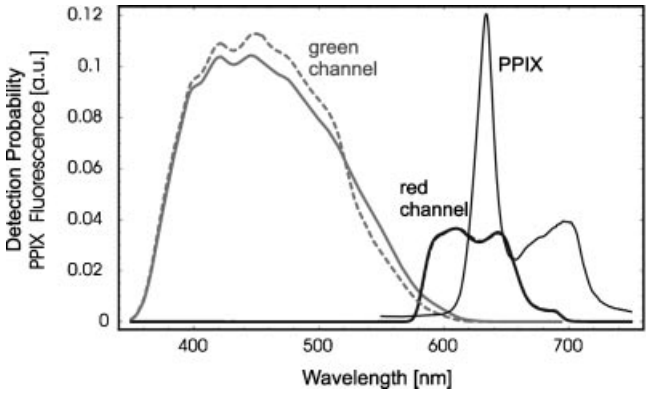

Fig. 2. Spectral sensitivity of the green channel and the red channel for the intensity (solid line) and lifetime (dotted line) imaging. The protoporphyrin IX emission spectrum is shown for comparison. The fluorescence emission was measured at 400 nm excitation using CCRF-CEM human leukemia cells following 4 hours incubation with 1 mM ALA.

intraperitoneal administration of 5-ALA and coronal sections were performed at the site of the implantation, white light illumination showed the distorted anatomy, the loss of normal white and gray matter structures of mouse brain and the increased tissue volume at the site of the tumor implantation. The tumor tissue with light yellow to gray color was difficult to discriminate from native gray matter. UV illumination demonstrated a prominent red fluorescence of the tumor mass and a less intense pink fluorescence at the tumor to deep white matter border and the corpus callosum (Fig. 3). The contralateral hemisphere showed no enhanced fluorescence. Multiphoton microscopy of the native coronal brain section at 750 nm excitation using the green channel showed the highly cellular tumor mass of the G-112 glioma with low signal intensity nuclei and a granular high signal intensity cytoplasm. Normal mouse brain of the contralateral hemisphere showed low signal intensity with few low intensity cellular nuclei and a homogenous low intensity signal of the parenchyma. At 810 nm excitation in the red channel the tumor tissue showed a detailed structure of low intensity cellular nuclei, strongly fluorescing cytoplasmic areas, but also signal intense extracellular spaces. Because of the strongly contrasted cellular elements, lacunar structures within the tumor parenchyma became more prominent. The normal brain parenchyma of the contralateral hemisphere showed very low intensity fluorescence. No cellular or other tissue structures could be discriminated. The analysis of the intensity of fluorescence of solid tumor and normal brain parenchyma demonstrated a maximum of the tumor/brain ratio of fluorescence intensity between 780 and 810 nm excitation (Fig. 4A). At 800–810 nm excitations the resolution of the intratumoral microstructure and a high fluorescence intensity ration of tumor/brain provided best diagnostic information (Fig. 4B). A comparison of

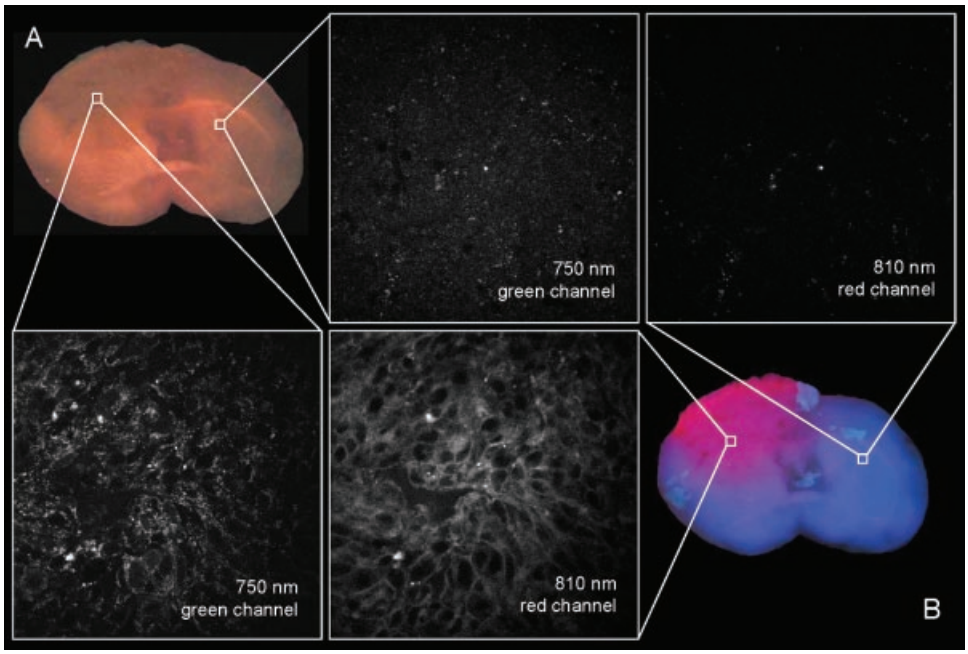

Fig. 3. **A**: White light image of a coronal section of a G-112 experimental glioma bearing mouse brain explanted 4 hours after intraperitoneal administration of 5-ALA. Multiphoton microscopy at 750 nm excitation using the green channel of the photomultiplier showed autofluorescence of the highly cellular tumor mass and a homogenous low intensity signal of the normal brain parenchyma. **B**: UV illumination showed red fluorescence of the tumor mass, but no enhanced fluorescence of normal brain. At 810 nm excitation using the red channel the histo-architecture of tumor tissue showed in detail with low intensity cellular nuclei, strongly fluorescing cytoplasmic areas, and signal intense extracellular spaces.

autofluorescence imaging and imaging of 5-ALA induced PpIX fluorescence of experimental G-112 gliomas showed that autofluorescence imaging at 750 nm excitation displayed the highly cellular tumor based on autofluorescence intensity as well as the characteristic microstructure. The tumor/brain interface could be identified based on the high density of low signal intensity tumor cell nuclei, the high signal intensity of the cytoplasm of tumor cells and the homogeneous and low intensity signal of normal brain (Fig. 5 lower panel). Autofluorescence imaging also identified some signal intense structures of normal brain such as the choroids plexus and the ventricular ependyma, which based on their anatomical characteristics, could be easily discriminated from tumor. Optimized detection of PpIX fluorescence in the red channel using 810 nm excitation showed the intense fluorescence of the cytoplasm of tumor cells within solid tumor. Interestingly, brain parenchyma immediately adjacent to invading tumor also showed high signal intensity whereas normal brain parenchyma of the contralateral hemisphere showed little fluorescence (Fig. 5 middle panel). The choroids plexus and the ventricular ependyma (data not shown) showed no 5-ALA induced fluorescence. Images obtained at 810 nm excitation in the green channel were of no diagnostic value except as negative control (Fig. 5 upper panel).

Fluorescence Lifetime Imaging of Protoporphyrin IX Fluorescence in Experimental Gliomas

The analysis of autofluorescence lifetime distributions in mouse brain excited at 750 nm demonstrated fluorescence lifetimes that varied depending on the brain region. Highly metabolic tissues such as the choroids plexus or ependymal cells of the ventricular system showed longer lifetimes of the autofluorescence signal compared to white or gray matter. In experimental gliomas tumor cells consistently showed significantly prolonged lifetimes (1,600–1,800 ps) compared to white or gray matter (approximately 1,500 ps) [25].

When the fluorescence lifetime of brain and brain tumor tissue was analyzed after intraperitoneal 5-ALA administration to experimental animals bearing U87 or G-112

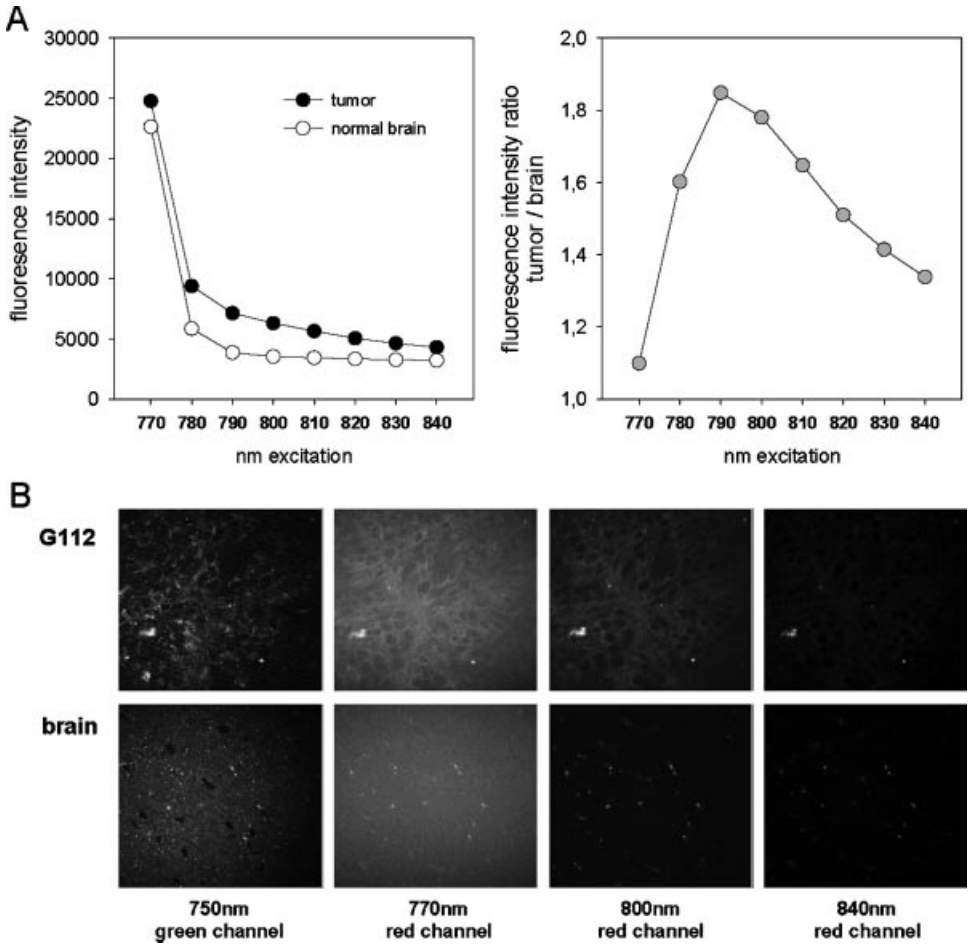

Fig. 4. Intensity analysis of solid tumor and normal brain parenchyma of 5-aminolevulinic acid induced fluorescence. A maximum of the tumor/brain ratio of fluorescence intensity occurred at 780–810 nm excitation (**A**). At 800–810 nm excitations the resolution of the intratumoral microstructure provided best diagnostic information (**B**).

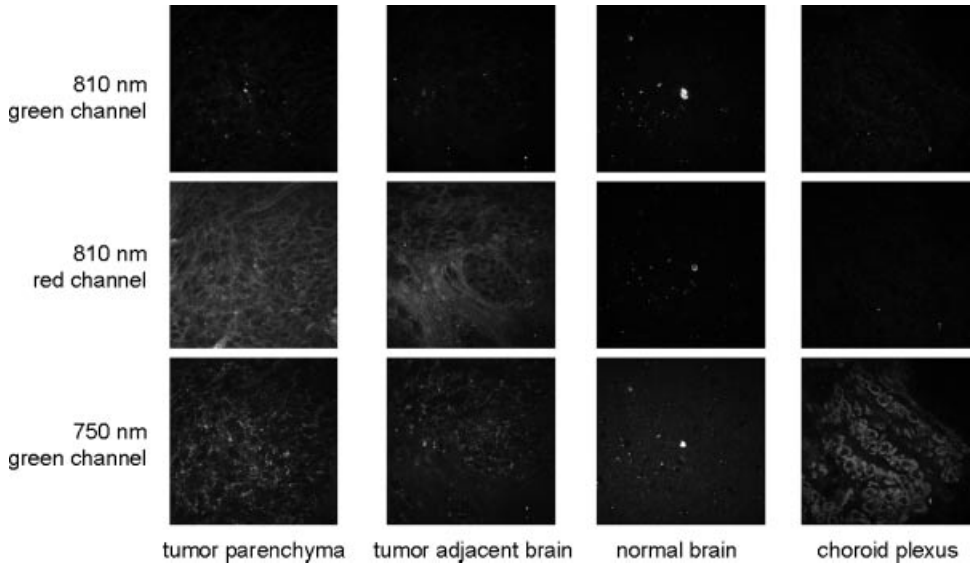

Fig. 5. Analysis of the tumor/brain interface and normal brain of 5-aminolevulinic acid induced fluorescence in invasive G-112 experimental gliomas in an orthotopic mouse model. **Lower panel**: Autofluorescence imaging at 750 nm in the green channel identified signal intense tumor cells neighboring low intensity normal brain parenchyma, but also identified some signal intense elements of normal brain such as the choroids plexus. Optimized detection of PpIX fluorescence in the red channel using 810 nm excitation showed the intense fluorescence of the cytoplasm of tumor cells and adjacent brain but the choroids plexus showed no 5-ALA induced fluorescence (**middle panel**). Images obtained at 810 nm excitation in the green channel were of no diagnostic value except as negative control (**upper panel**).

gliomas, excitation at 750 nm in the green channel, which allowed optimal detection of autofluorescence, showed the fluorescence lifetime of tumor adjacent brain <2,000 ps whereas the average fluorescence lifetimes of the cytoplasm of tumor cells ranged from 3,000 to 5,000 ps. Excitation at 810 nm and detection using the red channel filters with the red-sensitive photomultiplier showed the prominent fluorescence of the cytoplasmic PpIX in tumor cells but low signal intensity within tumor adjacent brain (Fig. 6). The fluorescence lifetime of normal brain was approximately 1,800 ps, ranging from 800 to 2,000 ps. Mean PpIX fluorescence lifetimes of the cytoplasm of tumor cells in six U87 tumor specimens were 2,871.8 ps $\pm$ 77.0 (vs. six specimens of normal contralateral brain 1,860.9 $\pm$ 57.4; $P<0.001$). In six specimens of G-112 gliomas the mean PpIX fluorescence lifetimes were 3,244.8 $\pm$ 110.8 (vs. six specimens of normal contralateral brain 1,805.2 $\pm$ 67.6; $P<0.001$). Gating of the color coding (red <1,900 ps, green >2,300 ps) resulted in a clear delineation of tumor versus adjacent brain in both U87 and G-112 tumors.

DISCUSSION

High tumor to normal brain fluorescence ratios of 5-ALA induced PpIX fluorescence have been demonstrated for experimental brain tumors such as the C6 gliomas [4]. Even though the ability of 5-ALA to cross the intact blood-brain barrier is limited due to its hydrophilic nature, the temporal course of porphyrin accumulation in C6 glioma tissue was found similar to other organ systems lacking a blood-brain barrier with highest fluorescence levels 3–6 hours after systemic administration of 5-ALA. This has been attributed to the disruption of the blood-brain barrier within malignant glioma tissue. Similar to findings in our study high fluorescence of the tumor periphery has been described as well as positive labeling of single invasive cells found in adjacent brain with a presumably intact blood-brain barrier [4]. Possible explanations may be that 5-ALA is carried by the bulk flow of edema from the tumor to the adjacent brain were it may be metabolized by invasive cells. In our study a relatively high dose of 5-ALA was used, which may have resulted in unspecific fluorescence of tumor adjacent brain possibly due to release of PpIX by tumor cells and distribution of the albumin and lipoprotein bound fluorophore by the bulk flow of edema. High doses of 5-ALA also may lead to accumulation of PpIX in plasma, which may result in low-level blood-borne fluorescence of normal tissue (discussed in Ref. [4]). 5-ALA induced fluorescence in the central nervous system is not strictly limited to tumor. The choroids plexus and the basal pia have been shown to accumulate PpIX fluorescence [4,27]. Similar to the findings in this study, tumor adjacent white matter has been found to significantly accumulate PpIX fluorescence. This may be due to propagation of free porphyrins or protein conjugated porphyrins with the bulk flow of brain edema. However, in experimental systems the tumor adjacent fluorescence extended only for 1–2 mm into white matter. On the other hand the central portions of

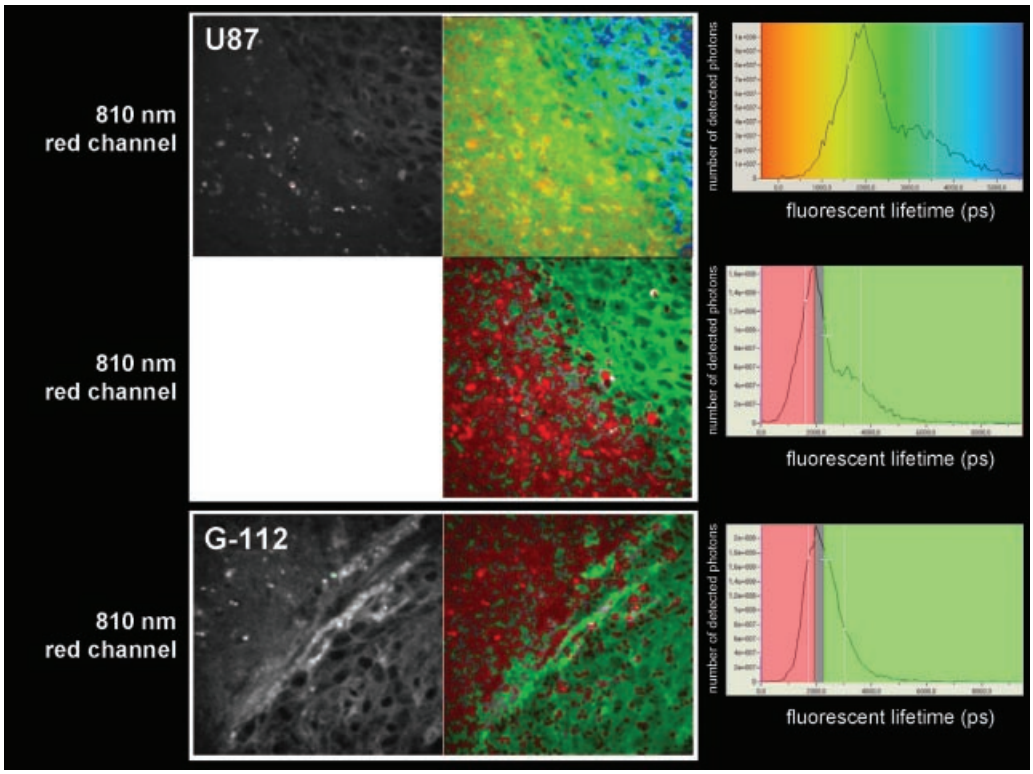

Fig. 6. Ex vivo fluorescence lifetime imaging of protoporphyrin IX fluorescence in experimental gliomas after intraperitoneal 5-ALA administration to experimental animals bearing U87 or G-112 gliomas.

experimental gliomas and the central necrosis of human malignant gliomas may not show 5-ALA induced fluorescence possibly due to the lack of sufficient perfusion or the lack of viable tumor cells. In this study we have used the contrasting effect of 5-ALA induced fluorescence to enhance the sensitivity of tumor cell detection by multiphoton microscopy, which allows a subcellular resolution of native tissues in vivo. Two-photon imaging of PpIX in cells [28] and tissues [29] has been reported before, however, difficulties of the necessity to suppress the strong excitation radiation have been encountered, because a red sensitive photomultiplier has to be used, which also is sensitive for the excitation radiation. Unlike in one photon excited fluorescence imaging, which provides good contrast of the PpIX and the autofluorescence, in our experiments using two photon excitation only a ratio of two could be achieved. The contrast was limited in parts by residual excitation light and by tissue autofluorescence excited at 800 nm. Multiphoton microscopy of experimental gliomas in mouse brain has demonstrated that a detailed image of the normal brain histoanatomy may be obtained in native tissue using the green channel of a standard photomultiplier, at an excitation wavelength of 750 nm [23]. Based on autofluorescence intensity images the histoarchitecture of cortex, white matter, fiber tracts within the basal ganglia or the ependyma can be readily identified [25]. Experimental gliomas on multiphoton intensity images can be identified because of their high cellularity and high autofluorescence of the tumor cell's cytoplasm contrasting with the low signal intensity nuclei. In biopsies taken from human brain tumors or the wall of resection cavities after surgical removal of malignant gliomas the density of tumor cells, representing, the degree of tumor infiltration could be determined based on the same parameters [Kantelhardt et al., manuscript in preparation]. The analysis of fluorescence lifetimes showed that highly metabolic tissues within normal brain for example the ependyma and the choroids plexus showed long lifetimes of autofluorescence. The highly proliferative experimental glioma tissue showed significantly longer fluorescence lifetimes than normal cortex or white matter and also exceeded those of the ependyma and choroids plexus. Similar findings were obtained for biopsies of human brain tumors. The analysis of the excitation wavelength to fluorescence lifetime showed that for cells derived from different tissues characteristic profiles may be obtained. The excitation to fluorescence lifetime profiles of glioma cells were found different from cells derived from other malignant human tumors, suggesting that fluorescence lifetime spectroscopy may differentiate histotypes of cells based on the excitability of cell type specific endogenous chromophores, their chemical states, or their interaction with other biomolecules [23]. Characterization of the excitation to fluorescence lifetime profiles of biopsies from human gliomas

demonstrated that the degree of malignancy tended to positively correlate with fluorescence lifetimes, suggesting that the photochemical analysis of glioma tissue may offer significant diagnostic information [25]. The difference of the autofluorescence lifetimes allowed visualization of the tumor/brain interface by lifetime gated color coded images. However, the autofluorescence lifetimes of individual tumors both experimental and human varied significantly, which did not allow automated detection of the tumor/brain interface by constant lifetime gate settings. Detection of 5-ALA induced PpIX fluorescence in experimental gliomas by multiphoton microscopy allowed high contrast intensity imaging of the glioma histoarchitecture, which could be easily discriminated form normal brain. The long fluorescence lifetime of PpIX fluorescence allowed identification of the tumor/brain interface using constant settings, which may facilitate automated detection of tumor and normal brain. Therefore, intraoperative in vivo multiphoton microscopy of brain tissue conceptually could provide a high resolution non-invasive diagnostic tool, which in addition to structural information may also provide photochemical/functional information. Recent technical developments suggest that some principle problems of high numerical aperture imaging of intraoperative brain imaging, which moves following the respiratory and arterial cycle, can potentially be solved. Multiphoton microscopy scanner probes connected to optic fibers can be miniaturized, which facilitated in vivo imaging of the mouse central nervous system over extended periods of time [31]. König et al. [32] have recently demonstrated that multiphoton microscopy can be performed through optical rods. Such probes may be placed in direct contact to the target tissue and may offer solutions to the specific requirements of intraoperative high resolution optical brain imaging. Because the geometry of a typical resection cavity requires the analysis of larger surface areas high resolution imaging may only be feasible in areas were residual tumor is suspected. For the screening of larger areas of the resection edge we have recently demonstrated that lower resolution techniques such as optical coherence tomography can differentiate tumor tissue and normal brain based on the light attenuation profiles and the appearance of a prominent microstructure in tumor tissue [33]. Theoretically, multiphoton microscopy and optical coherence tomography can share similar light sources and may be applied through similar optical probes offering an opportunity to combine these modalities into one device. A combination of low and high resolution intraoperative imaging techniques may therefore be promising in screening large intaoperative resection cavities combined with an analysis at the subcellular level for areas that show a loss of the light attenuation pattern of normal brain or occurrence of an abnormal microstructure.

REFERENCES

1. Uehlinger P, Zellweger M, Wagnieres G, Juillerat-Jeanneret L, van den Bergh H, Lange N. 5-Aminolevulinic acid and its derivatives: Physical chemical properties and protoporphyrin IX formation in cultured cells. J Photochem Photobiol B 2000;54(1):72–80.
2. Hebeda KM, Saarnak AE, Olivo M, Sterenborg HJ, Wolbers JG. 5-Aminolevulinic acid induced endogenous porphyrin fluorescence in 9L and C6 brain tumours and in the normal rat brain. Acta Neurochir (Wien) 1998;140(5):503–512.
3. Stummer W, Novotny A, Stepp H, Goetz C, Bise K, Reulen HJ. Fluorescence-guided resection of glioblastoma multiforme by using 5-aminolevulinic acid-induced porphyrins: A prospective study in 52 consecutive patients. J Neurosurg 2000;93:1003–1013.
4. Stummer W, Stocker S, Novotny A, Heimann A, Sauer O, Kempski O, Plesnila N, Wietzorrek J, Reulen HJ. In vitro and in vivo porphyrin accumulation by C6 glioma cells after exposure to 5-aminolevulinic acid. J Photochem Photobiol B 1998;45(2–3):160–169.
5. Stummer W, Stocker S, Wagner S, Stepp H, Fritsch C, Goetz C, Goetz AE, Kiefmann R, Reulen HJ. Intraoperative detection of malignant gliomas by 5-aminolevulinic acid-induced porphyrin fluorescence. Neurosurgery 1998;42(3):518–525.
6. Angell-Petersen E, Spetalen S, Madsen SJ, Sun CH, Peng Q, Carper SW, Sioud M, Hirschberg H. Influence of light fluence rate on the effects of photodymamic therapy in an orthotopic rat glioma model. J Neurosurg 2006;104(1):109–117.
7. Stummer W, Stepp H, Moller G, Ehrhardt A, Leonhard M, Reulen HJ. Technical principles for protoporphyrin-IX-fluorescence guided microsurgical resection of malignant glioma tissue. Acta Neurochir (Wien) 1998;140(10):995–1000.
8. Bogaards A, Varma A, Collens SP, Lin A, Giles A, Yang VX, Bilbao JM, Lilge LD, Muller PJ, Wilson BC. Increased brain tumor resection using fluorescence image guidance in a preclinical model. Lasers Surg Med 2004;35(3):181–190.
9. Utsuki S, Oka H, Sato S, Shimizu S, Suzuki S, Tanizaki Y, Kondo K, Miyajima Y, Fujii K. Histological examination of false positive tissue resection using 5-aminolevulinic acid-induced fluorescence guidance. Neurol Med Chir (Tokyo) 2007;47(5):210–213; discussion 213–214.
10. Stummer W, Pichlmeier U, Meinel T, Wiestler OD, Zanella F, Reulen HJ, ALA-Glioma Study Group. Fluorescence-guided surgery with 5-aminolevulinic acid for resection of malignant glioma: A randomised controlled multicentre phase III trial. Lancet Oncol 2006;7(5):392–401.
11. Filbeck T, Roessler W, Knuechel R, Straub M, Kiel HJ, Wieland WF. Clinical results of the transurethreal resection and evaluation of superficial bladder carcinomas by means of fluorescence diagnosis after intravesical instillation of 5-aminolevulinic acid. J Endourol 1999;13(2):117–121.
12. Kriegmair M, Baumgartner R, Knuchel R, Stepp H, Hofstadter F, Hofstetter A. Detection of early bladder cancer by 5-aminolevulinic acid induced porphyrin fluorescence. J Urol 1996;155(1):105–109.
13. Riedl CR, Plas E, Pfluger H. Fluorescence detection of bladder tumors with 5-amino-levulinic acid. J Endourol 1999;13(10):755–759.
14. Leunig A, Betz CS, Mehlmann M, Stepp H, Arbogast S, Grevers G, Baumgartner R. A pilot series demonstrating fluorescence staining of laryngeal papilloma using 5-aminolevulinic acid. Laryngoscope 2000;110:1783–1785.
15. Wang I, Clemente LP, Pratas RM, Cardoso E, Clemente MP, Montan S, Svanberg S, Svanberg K. Fluorescence diagnostics and kinetic studies in the head and neck region utilizing low-dose delta-aminolevulinic acid sensitization. Cancer Lett 1999;135:11–19.
16. Baumgartner R, Huber RM, Schulz H, Stepp H, Rick K, Gamarra F, Leberig A, Roth C. Inhalation of 5-aminolevulinic acid: A new technique for fluorescence detection of early stage lung cancer. J Photochem Photobiol B 1996;36:169–174.
17. Hillemanns P, Weingandt H, Baumgartner R, Diebold J, Xiang W, Stepp H. Photodetection of cervical intraepithelial neoplasia using 5-aminolevulinic acid-induced porphyrin fluorescence. Cancer 2000;88:2275–2282.
18. Malik E, Berg C, Meyhofer-Malik A, Buchweitz O, Moubayed P, Diedrich K. Fluorescence diagnosis of endometriosis using 5-aminolevulinic acid. Surg Endosc 2000;14:452–455.

19. Löning M, Diddens H, Kupker W, Diedrich K, Hüttmann G. Laparoscopic fluorescence detection of ovarian carcinoma metastases using 5-aminolevulinic acid-induced protoporphyrin IX. Cancer 2004;100:1650–1656.
20. Löning M, Diddens H, Holl-Ulrich K, Löning U, Küpker W, Diedrich K, Hüttmann G. Fluorescence staining of human ovarian cancer tissue following application of 5-aminolevulinic acid: Fluorescence microscopy studies. Lasers Surg Med 2006;38:549–554.
21. Messmann H. 5-Aminolevulinic acid-induced protoporphyrin IX for the detection of gastrointestinal dysplasia. Gastrointest Endosc Clin N Am 2000;10:497–512.
22. Ackermann G, Abels C, Karrer S, Baumler W, Landthaler M, Szeimies RM. Fluorescence-assisted biopsy of basal cell carcinomas. Hautarzt 2000;51:920–924.
23. Leppert J, Krajewski J, Kantelhardt SR, Schlaffer S, Petkus N, Reusche E, Huttmann G, Giese A. Multiphoton excitation of autofluorescence for microscopy of glioma tissue. Neurosurgery 2006;58(4):759–767.
24. König K. Multiphoton microscopy in life sciences. J Microsc 2000;200(Pt 2):83–104.
25. Kantelhardt SR, Leppert J, Krajewski J, Petkus N, Reusche E, Tronnier VM, Huttmann G, Giese A. Imaging of brain and brain tumor specimens by time-resolved multiphoton excitation microscopy ex vivo. Neuro-oncol 2007;2:103–112.
26. Becker W, Bergmann A, König K, Tirlapur U. Picosecond fluorescence lifetime microscopy by TCSP imaging. Proc SPIE 2001;4262:414–419.
27. Novotny A, Xiang J, Stummer W, Teuscher NS, Smith DE, Keep RF. Mechanisms of 5-aminolevulinic acid uptake at the choroid plexus. J Neurochem 2000;75:321–328.
28. Kendall CA, McCloskey K, Stone N, Barr H, Greenhalgh D. Multiphoton imaging in the detection of malignancy in the oesophagus. In: Wilson T, editor. Confocal, multiphoton, and nonlinear microscopic imaging: Proceedings of SPIE Vol. 5139. Wilson T, Ed. 2003. pp. 51–55.
29. Ganesan S, Elangovan M, Periasamy A. Kinetics and comparison of δ-aminolevulinic-acid-induced endogenous protoporphyrin-IX in single cell by steady state and multiphoton fluorescence imaging. In: Periasamy A, So PT, editors. Multiphoton microscopy in the biomedical sciences; proceedings of SPIE Vol. 4262. Periasamy A, So PTC, Eds. 2001. 263–267.
30. Kim D, Kim KH, Yazdanfar S, So PTC. High-speed handheld multiphoton multifoci microscopy. Multiphoton microscopy in the biomedical science IV, at Biomedical Optics 2001,San Jose, CA. SPIE Proc 2004;5323:267–272.
31. König K, Ehlers A, Riemann I, Schenkl S, Buckle R, Kaatz M. Clinical two-photon microendoscopy. Microsc Res Tech 2007;70:398–402.
32. Böhringer HJ, Boller D, Leppert J, Knopp U, Lankenau E, Reusche E, Hüttmann G, Giese A. Time domain and spectral domain optical coherence tomography in the analysis of brain tumor tissue. Laser Surg Med 2006;38:588–597.
33. Böhringer HJ, Lankenau E, Rohde V, Hüttmann G, Giese A. Optical coherence tomography or experimental neuroendoscopy. Minim Invasive Neurosurg 2006;49:269–275.